Supplementary Information

Table S1. The allometric equation of trees for estimating field AVWS.

Tree Species	Position	Empirical formula	Quote
Cypress	Branch	$W_b=0.0350*(D^2H)^{\wedge}(0.7119)$	[1]
	Stem	$W_s=0.0754*(D^2H)^{\wedge}(0.7934)$	
	Leaf	$W_l=0.0685*(D^2H)^{\wedge}(0.6583)$	
Locust	Branch	$Wb=58.6653*(D2H)^{\wedge}(0.18258)$	[5]
	Stem	$Ws=207.6566*(D2H)^{\wedge}(0.8112)$	
	Leaf	$Wl=11.7388*(D2H)^{\wedge}(0.6406)$	
Chinese pine	Branch	$Wb=0.0689*D^{\wedge}2.1435$	[2]
	Stem	$Ws=0.0967*D^{\wedge}2.126$	
	Leaf	$Wl=0.0133*D^{\wedge}2.4283$	
Fir	Branch	$Wb=0.0037*D^{\wedge}(2.7386)$	[3]
	Stem	$Ws=0.0405*D^{\wedge}(2.568)$	
	Leaf	$Wl=0.0014*D^{\wedge}(2.9302)$, D<40 cm $Wl=29.541*ln(D)-63.15$, D>40 cm	
Picea-Abies	Branch	$Wbranch=0.0037*D^{\wedge}2.7386$	[3]
	Stem	$Wsteam=0.0450*D^{\wedge}205860$	
	Leaf	$Wleaf=0.0014*D^{\wedge}2.9302$	
Poplar	Branch	$Wb=0.3521*D^{\wedge}(1.5212)$	[5]
	Stem	$Ws=0.1745*D^{\wedge}(2.1667)$	
	Leaf	$Wl=0.0008*D^{\wedge}(2.9066)$	
Oak tree	Branch	$Wb=0.0261*D^{\wedge}(2.4658)$	[5]

	Stem	Ws=0.0346*D^(2.6758)	
	Leaf	Wl=0.0004*D^(2.9285)	
Birch	Branch	Wbranch=12.853*D^0.3021	[4]
	Stem	Wsteam=22.426*D^0.385	
	Leaf	Wleaf=5.3765*D^0.3916	
Other broad leaved tree species	Branch	Wb=0.5261*(D)^(1.5945)	[5]
	Stem	Ws=0.0147*(D)^(2.8094)	
	Leaf	Wl=0.0987*(D)^(1.4916)	

Table S2. Sentinel-2 Satellite sensor parameters

Sensor	Band number	Band name	Wavelength (nm)	Resolution (meters)
MSI	1	Coastal aerosol	433-453	60
MSI	2	Blue	458-523	10
MSI	3	Green	543-578	10
MSI	4	Red	650-680	10
MSI	5	Vegetation Red Edge	698-713	20
MSI	6	Vegetation Red Edge	733-748	20
MSI	7	Vegetation Red Edge	773-793	20
MSI	8	NIR	785-900	10
MSI	8a	Narrow NIR	855-875	20
MSI	9	Water vapour	935-955	60
MSI	10	SWIR – Cirrus	1360-1390	60
MSI	11	SWIR-1	1565-1655	20
MSI	12	SWIR-2	2100-2280	20

Table S3. Landsat 8 Satellite sensor parameters

Sensor	Band number	Band name	Wavelength(nm)	Resolution (meters)
OLI	Band1	Coastal aerosol	430-450	30
	Band2	Blue	450-515	30
	Band3	Green	525-600	30
	Band4	Red	630-680	30
	Band5	NIR	845-885	30
	Band6	SWIR1	1560-1660	30
	Band7	SWIR2	2100-2300	30
	Band8	PAN	503-676	15
	Band9	Cirrus	1360-1390	30
TIRS	Band10	TIRS1	10600-11210	100
	Band11	TIRS2	11500-12500	100

Table S4. The statistics of the land cover in Jiuzhaigou National Nature Reserve

Type	Pixels (number)	Total area (ha)	Percentage
Snow	1763954	17639.54	27.12%
Water Body	9756	97.56	0.15%
Bare Soil	1171417	11714.17	18.01%
Coniferous Forest	1866762	18667.62	28.70%
Broad-leaved Forest	1036300	10363.00	15.93%
Mixed Forests	109295	1092.95	1.68%
Shrubwood	166204	1662.04	2.56%
Grassland	380568	3805.68	5.85%
Total	6504256	65042.56	1.00

Table S5. Vegetation indices to estimate AVWS.

Number	Vegetation Index Types	Calculation Formula	References
1	Perpendicular Vegetation Index	$PVI = \dfrac{R_{nir} - \alpha R_{red} - \beta}{\sqrt{\alpha^2 + 1}}$	[6]
2	Triangle Vegetation Index	$TVI = 0.5 \cdot [120 \cdot (R_{nir} - R_{green}) - 200 \cdot (R_{red} - R_{green})]$	[7]
3	Difference Vegetation Index	$DVI = R_{nir} - R_{red}$	[8]
4	Normalized Green-Blue Difference Index	$NGBDI = \dfrac{R_{green} - R_{blue}}{R_{green} + R_{blue}}$	[9]
5	Green-Blue Ratio Index	$GBRI = \dfrac{R_{green}}{R_{blue}}$	[10]
6	Atmospherically Resistant Vegetation Index	$ARVI = \dfrac{(R_{560} - R_{660})}{(R_{560} + R_{660} + R_{480})}$	[11]
7	Green-Red Ratio Index	$GRRI = \dfrac{R_{green}}{R_{red}}$	[12]
8	Specific Leaf Area Vegetation Index	$SLAVI = \dfrac{R_{nir}}{R_{red} + R_{mir}}$	[13]
9	Normalized Different Moisture Index	$NDMI = \dfrac{(R_{nir} - R_{swir1})}{(R_{nir} + R_{swir1})}$	[14]
10	Normalized Difference Infrared Index	$NDII = \dfrac{(R_{820} - R_{1600})}{(R_{820} + R_{1600})}$	[15]

Notes: Red, blue, green, NIR and Mir in the table represent the atmospheric corrected spectral reflectance in red band, blue band, green band, near infrared band and mid infrared band respectively.

Table S6. Texture indices to estimate AVWS.

Serial Number	Texture Features	Calculation Formula
1	Mean	$\displaystyle\sum_{i,j=0}^{n-1} i(P_{i,j})$
2	Variance	$\displaystyle\sum_{i,j=0}^{n-1} iP_{i,j}(i-Mean)^2$
3	Homogeneity	$\displaystyle\sum_{i,j=0}^{n-1} i\frac{P_{i,j}}{1+(i-j)^2}$
4	Contrast	$\displaystyle\sum_{i,j=0}^{n-1} iP_{i,j}(i-1)^2$
5	Dissimilarity	$\displaystyle\sum_{i,j=0}^{n-1} iP_{i,j}|(i-j)|$
6	Entropy	$\displaystyle\sum_{i,j=0}^{n-1} iP_{i,j}(-\ln P_{i,j})$
7	Second Moment	$\displaystyle\sum_{i,j=0}^{n-1} iP_{i,j}{}^2$
8	Correlation	$\displaystyle\sum_{i,j=0}^{n-1} iP_{i,j}\left[\frac{(i-Mean)(j-Mean)}{\sqrt{Variance_i \cdot Variance_j}}\right]$

Notes： i and j represent the row number and column number in the gray-level co-occurrence matrix, respectively. $P_{i,j}$ represents the pixel value of row i and column j in the gray-level co-occurrence matrix. n is the number of distinct gray levels in the quantized.
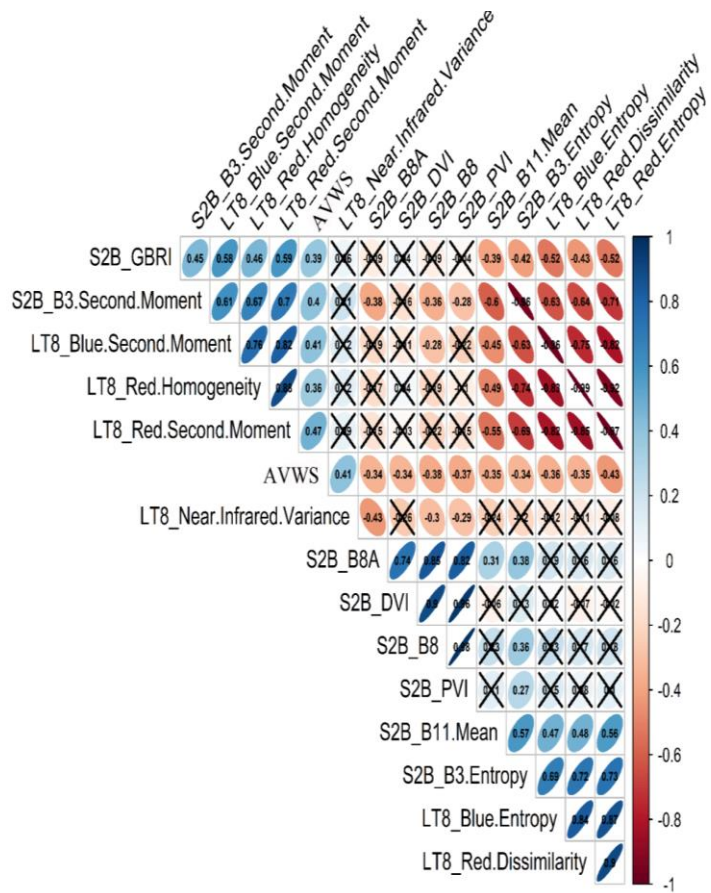
Table S7. The number of the variables input to the model.

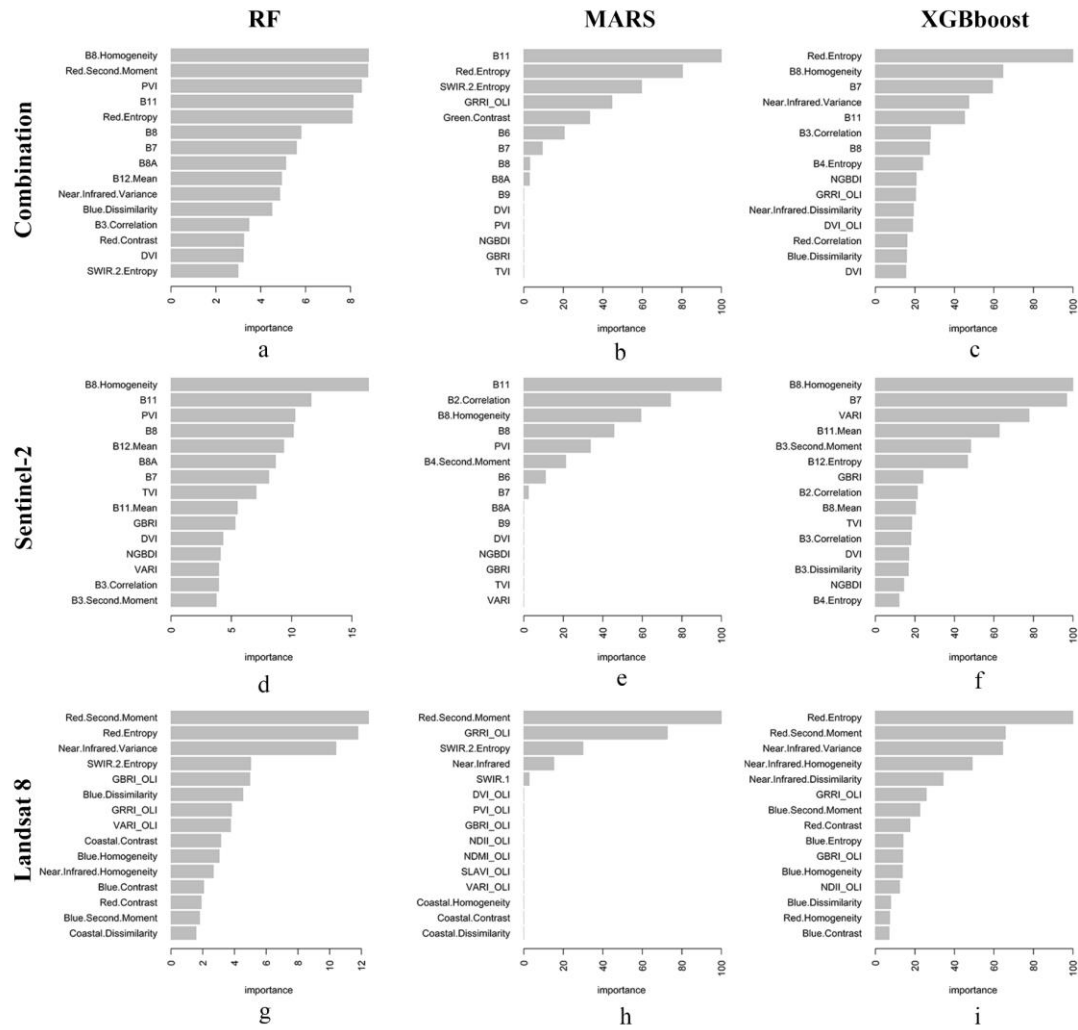| Dataset	Model	Number of input features
Sentinel-2	MARS	5
	RF	5
	XGB	6
Landsat 8	MARS	5
	RF	4
	XGB	3
Sentinel-2+Landsat 8	MARS	7
	RF	6
	XGB	6
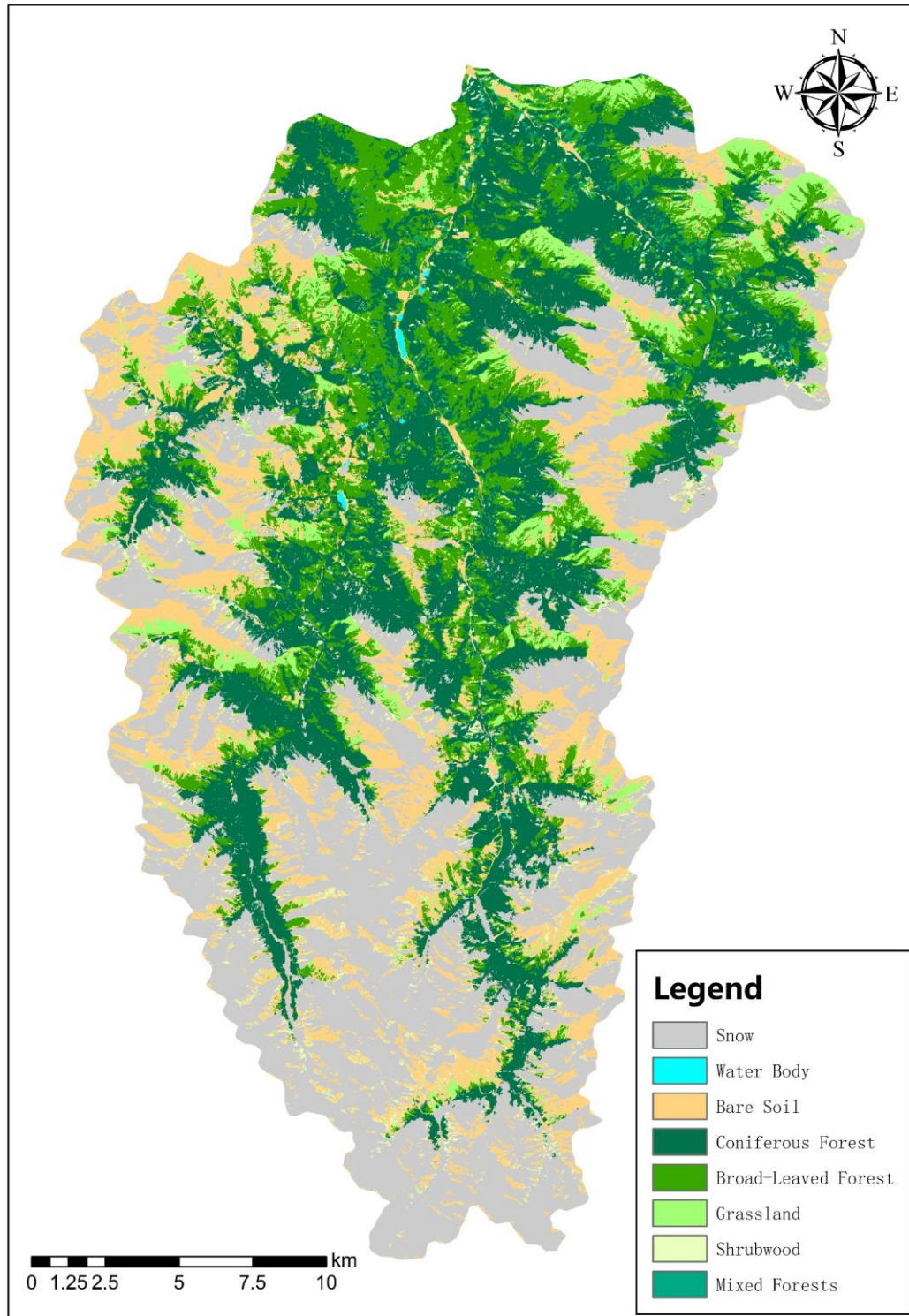
Figure S1. Classification of land cover in the study area

Figure S2. The correlations between AVWS and the variables of Sentinel-2B and Landsat 8 OLI. The 15 variables most correlated with AVWS were showed at a significance of $p < 0.05$.

Figure S3. The Importance of variables from three dataset (Landsat 8, Sentinel-2 and their combination) using RF, XGB, and MARS algorithms.
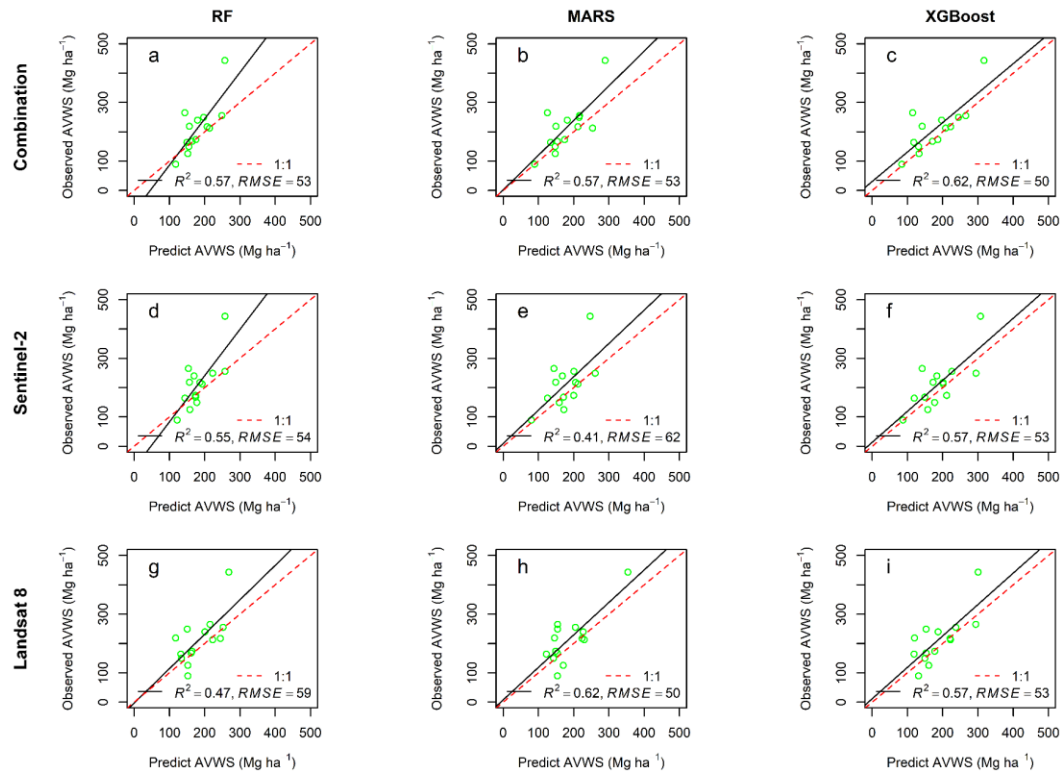
Figure S4. The correlation between predicted and observed aboveground vegetation water storage (AVWS) of coniferous forest using different modelling approaches (XGBoost, RF and MARS) and satellite images (Landsat 8 and Sentinel-2).
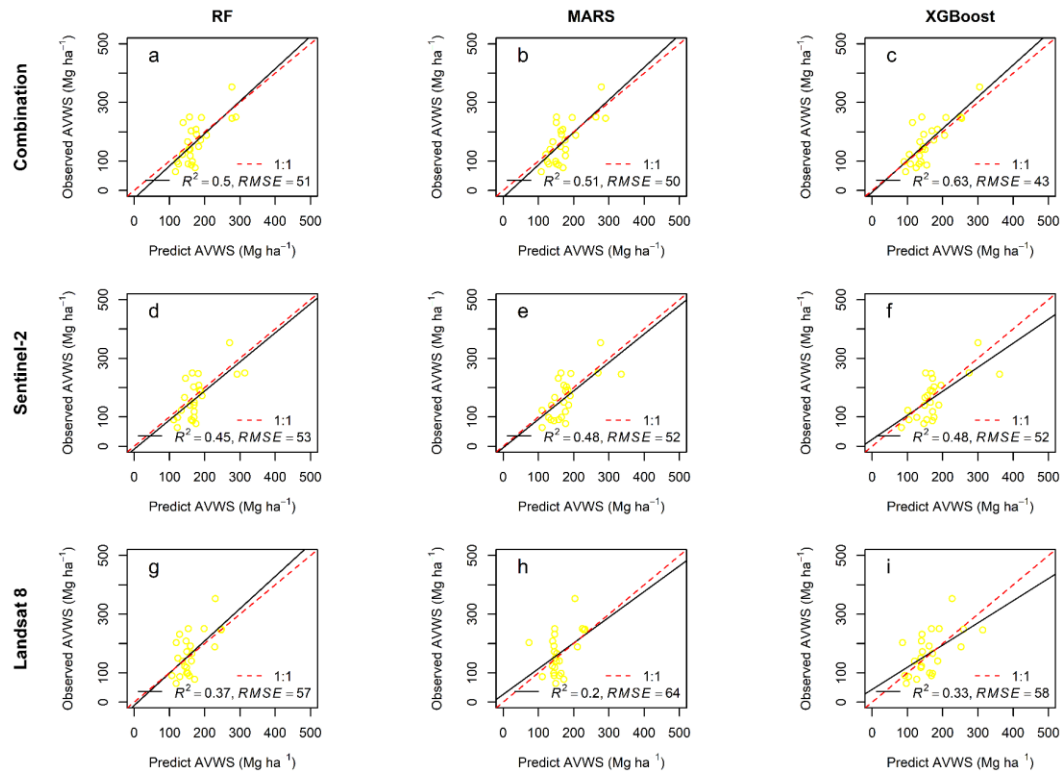
Figure S5. The correlation between predicted and observed aboveground vegetation water storage (AVWS) of mixed forest using different modelling approaches (XGBoost, RF and MARS) and satellite images (Landsat 8 and Sentinel-2).
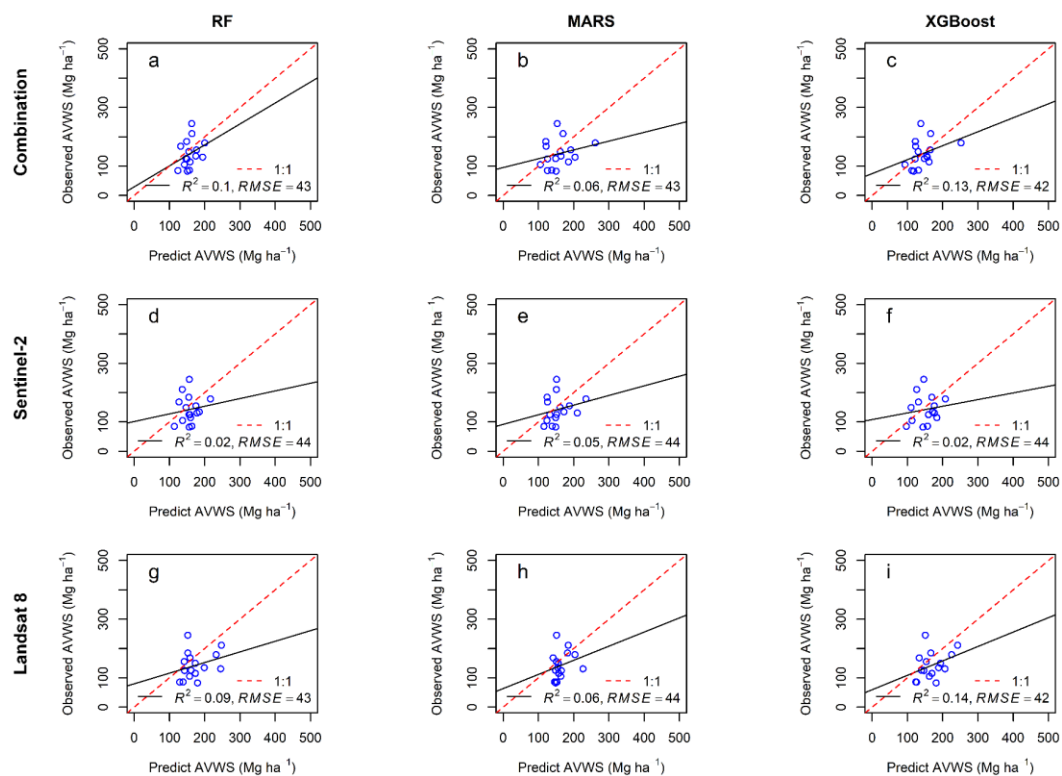
Figure S6. The correlation between predicted and observed aboveground vegetation water storage (AVWS) of broadleaved forest using different modelling approaches (XGBoost, RF and MARS) and satellite images (Landsat 8 and Sentinel-2).

References

1. Shi, P.L.; Zhong, Z.C.; Li, X.G. A STUDY ON THE BIOMASS OF ALDER AND CYPRESS ARTIFICIAL MIXED FOREST IN SICHUAN. *Acta Phytoecologica Sinica*.**1996**, 20, 524-533.
2. Kong, W.J.; Zheng, Z. The Aboveground Biomass and Net Primary Productivity of Degraded and Artificial Communities in Maoxian, Upper Reach of Minjiang River. *JOURNAL OF MOUNTAIN SCIENCE*.**2004**, 22, 445-450.
3. Luo, T.X.; Shi, P.L.; Luo, J.; Ou, Y.H. DISTRIBUTION PATTERNS OF ABOVEGROUND BIOMASS IN TIBETAN ALPINE VEGETATION TRANSECTS. *Acta Phytoecologica Sinica*.**2002**,26,668-676.
4. Li, W.B. Study on Biomass compositions of Principal vegetations and their relationships in the Dagou Valley of the upper Minjiang River. Master Dissertation, SouthwestUniversity,China,2007.
5. Luo, Y.J.; Wang, X.K.; Lu, f.*COMPREHENSIVE DATABASE OF BIOMASS REGRESSIONS FOR CHINA`S TREE SPECIES*. China Forestry Publishing House:Beijing, China,2015.
6. Roujean, J.L.; Breon, F.M. ESTIMATING PAR ABSORBED BY VEGETATION FROM BIDIRECTIONAL REFLECTANCE MEASUREMENTS. *Remote Sensing of Environment*. **1995** ,51,375-384.
7. Broge, N.H.; Leblanc, E. Comparing prediction power and stability of broadband and hyperspectral vegetation indices for estimation of green leaf area index and canopy chlorophyll density. *Remote Sensing of Environment*. **2001** ,76,156-172.
8. Jordan, C.F. Derivation of leaf-area index from quality of light on the forest floor. *Ecology*. **1969**,50,663-666.
9. Hunt, E.R.; Cavigelli, M.; Daughtry, C.S.T. Evaluation of Digital Photography from Model Aircraft for Remote Sensing of Crop Biomass and Nitrogen Status. *Precision Agriculture*. **2005**,6,359-378.
10. Sellaro, R.; Crepy, M.; Ariel Trupkin, S. Cryptochrome as a Sensor of the Blue/Green Ratio of Natural Radiation in Arabidopsis. *Plant Physiology*. **2010**,154,401-409.
11. Kaufman, Y.J.; Tanre, D. Atmospherically resistant vegetation index (ARVI) for EOS-MODIS. *IEEE transactions on Geoscience and Remote Sensing*. **1992**,;30(2):261-270.
12. Rondeaux, G.; Steven, M.; Baret, F. Optimization of soil-adjusted vegetation indices. *Remote Sensing of Environment*. **1996**,55,95-107.
13. Lymburner, L.; Beggs, P.J.; Jacobson, C.R. Estimation of canopy-average surface-specific leaf area using Landsat TM data. *Photogrammetric Engineering and Remote Sensing*. **2000**,66,183-192.
14. Hardisky, M.A.; Klemas, V.; Smart, M. The influence of soil salinity, growth form, and leaf moisture on the spectral radiance of Spartina alterniflora canopies. *Pho-togrammetric Engineering and Remote Sensing*. **1983**,49,77-83.
15. Hunt Jr, E.R.; Rock, B.N. Detection of changes in leaf water content using near-and middle-infrared reflectances. *Remote sensing of environment*. **1989**,30,43-54.